

Wavefronts in dissipative anisotropic media: Comparison of the plane-wave theory with numerical modeling

José M. Carcione*, Gerardo Quiroga-Goode*, and Fabio Cavallini*

ABSTRACT

In a previous work, Carcione investigated the characteristics of wavefronts in a dissipative anisotropic (orthorhombic) medium by means of time-harmonic, homogeneous, plane-wave analysis. Here, we extend the theoretical analysis to a monoclinic medium and perform numerical experiments to investigate the transient response. Given a line source the forward modeling algorithm computes pure shear waves in the symmetry plane of the medium. The results of the theoretical analysis agree with those of our transient wave simulation. For instance, the onset of the wavefield coincides with the theoretical wavefront calculated with the unrelaxed (high-frequency limit) energy velocity. Moreover, while the wavefronts computed with the theoretical envelope and energy velocities coincide practically with a numerical evaluation of the energy location, using the group velocity yields a wrong prediction. Finally, as an interesting example, we present a medium where the wave behaves isotropically (cylindrical wavefronts) at a given frequency, but is strongly anisotropic at the low- and high-frequency limits.

INTRODUCTION

Research on harmonic and transient wave propagation in anisotropic and dissipative media is relatively recent (Hosten et al., 1987; Carcione, 1990; Arts, 1993; Carcione and Cavallini, 1993a, b; Le et al., 1994). The differences between elastic and anelastic wavefields can be substantial; for instance, in shallow unconsolidated sediments and reservoir rocks. In an elastic medium, the wavefront is defined as the envelope of the family of planes that makes the phase of the plane waves zero. The velocity of the envelope of plane waves coincides with the energy and group velocities, but in dissipative anisotropic media these three velocities are different (Carcione, 1994).

Pulses generated in a homogeneous anelastic medium are assumed to be a superposition of time-harmonic homogeneous viscoelastic plane waves, for which the propagation and attenuation directions coincide. Therefore, we compare theoretical results, based on this type of wave, with numerical wavefronts of pure shear waves propagating in the symmetry plane of a homogeneous monoclinic medium.

THEORETICAL RESULTS

The following quantities describe the wave propagation properties of time-harmonic plane shear waves in the (x, z) symmetry plane of a viscoelastic monoclinic medium:

- c_{44}, c_{66}, c_{46} : elastic constants at infinite frequency;
- p_{44}, p_{66}, p_{46} : frequency-dependent complex stiffnesses;
- $\tau_{\epsilon}^{(1)}, \tau_{\sigma}^{(1)}$: relaxation times along the z-axis;
- $\tau_{\epsilon}^{(2)}, \tau_{\sigma}^{(2)}$: relaxation times along the x-axis;
- ρ : density.

In addition, we use the following symbols:

- t : time variable;
- ω : angular frequency;
- f : frequency;
- θ : propagation angle;
- $\hat{\mathbf{k}} = (\sin \theta, \cos \theta) = (\ell_x, \ell_z)$: propagation direction;
- $P_x = p_{66} \ell_x + p_{46} \ell_z$,
- $P_z = p_{44} \ell_z + p_{46} \ell_x$.

Generalizing to monoclinic media the results obtained in Carcione (1994) for orthorhombic media, we get

Complex velocity:

$$V = \left(\frac{p_{66} \ell_x^2 + p_{44} \ell_z^2 + 2p_{46} \ell_x \ell_z}{\rho} \right)^{1/2}. \quad (1)$$

Slowness vector:

$$\mathbf{s} = \text{Re}[V^{-1}] \hat{\mathbf{k}}. \quad (2)$$

Manuscript received by the Editor December 12, 1994; revised manuscript received August 4, 1995.
 *Osservatorio Geofisico Sperimentale, P.O. Box 2011 Opicina, I-34016 Trieste, Italy.
 © 1996 Society of Exploration Geophysicists. All rights reserved.

Attenuation vector:

$$\boldsymbol{\alpha} = -\omega \text{Im}[V] \hat{\mathbf{k}}. \quad (3)$$

Phase velocity vector:

$$\mathbf{V}_p = (\text{Re}[V^{-1}])^{-1} \hat{\mathbf{k}}. \quad (4)$$

Quality factor:

$$Q = \text{Re}[V^2] / \text{Im}[V^2]. \quad (5)$$

Envelope velocity:

$$\mathbf{v}_{\text{env}} = \frac{1}{\rho} \left\{ 1 + V_p^2 \left(\text{Re} \left[\frac{(p_{66} - p_{44}) \ell_x \ell_z + p_{46} (\ell_z^2 - \ell_x^2)}{\rho V^3} \right] \right)^2 \right\}^{1/2}. \quad (6)$$

Energy velocity:

$$\mathbf{V}_e = \frac{V_p}{\text{Re}[V]} \left\{ \text{Re} \left[\frac{1}{\rho V} (p_x \hat{\mathbf{e}}_x + p_z \hat{\mathbf{e}}_z) \right] \right\}. \quad (7)$$

Group velocity:

$$\mathbf{V}_g = -2 \hat{\mathbf{e}}_x \left(\text{Re} \left[\frac{D}{p_x V} \right] \right)^{-1} - 2 \hat{\mathbf{e}}_z \left(\text{Re} \left[\frac{D}{p_z V} \right] \right)^{-1}, \quad (8)$$

where

$$D = \omega (p'_{66} \ell_x^2 + p'_{44} \ell_z^2) - 2\rho V^2, \quad (9)$$

and the prime denotes the derivative with respect to the angular frequency. As in Carcione (1994), we define the wavefront as the locus of the tip of the energy velocity vector, and find that the envelope velocity closely approaches the energy velocity for all propagation directions. On the other hand, the group velocity can be used to describe the wavefront only for low-loss media. Moreover, the analysis reveals that differences in attenuation along the principal axes strongly influence the velocities.

EXAMPLES

Constitutive law

We consider a monoclinic medium with $p_{44} = c_{44} M^{(1)}$, $p_{66} = c_{66} M^{(2)}$, and $p_{46} = c_{46}$, where

$$M^{(m)} = \frac{\tau_\sigma^{(m)}}{\tau_\epsilon^{(m)}} \left[\frac{1 + i\omega\tau_\epsilon^{(m)}}{1 + i\omega\tau_\sigma^{(m)}} \right], \quad m = 1, 2, \quad (10)$$

are dimensionless complex moduli representing standard linear solid elements. Note that if $\omega \rightarrow \infty$, then $M^{(m)} \rightarrow 1$, and c_{44} , c_{66} , and c_{46} represent the high-frequency limit elastic constants. The quality factors for homogeneous waves along the z and x axes are

$$Q^{(m)} = Q_0^{(m)} \left[\frac{1 + (\omega\tau_0^{(m)})^2}{2\omega\tau_0^{(m)}} \right], \quad (11)$$

where

$$Q_0^{(m)} = \frac{2\tau_0^{(m)}}{\tau_\epsilon^{(m)} - \tau_\sigma^{(m)}} \quad (12)$$

and

$$\tau_0^{(m)} = \sqrt{\tau_\epsilon^{(m)} \tau_\sigma^{(m)}} \quad (13)$$

(Carcione, 1994). The curve $Q^{(m)}(\omega)$ has its minimum at $\omega_0^{(m)} = 1/\tau_0^{(m)}$ and the value of $Q^{(m)}$ at the minimum is $Q_0^{(m)}$. The relaxation times are obtained from equations (12) and (13):

$$\tau_\epsilon^{(m)} = \frac{\tau_0^{(m)}}{Q_0^{(m)}} (\sqrt{Q_0^{(m)2} + 1} + 1), \quad (14)$$

$$\tau_\sigma^{(m)} = \frac{\tau_0^{(m)}}{Q_0^{(m)}} (\sqrt{Q_0^{(m)2} + 1} - 1). \quad (15)$$

Wave equation

The wave equation used here is the generalized version of the *SH* equation, including anisotropy and attenuation effects, introduced in Carcione and Cavallini, 1993b. For instance, for one dissipation mechanism, the wave equation (for the displacement u and strain memory variables $e^{(1)}$ and $e^{(2)}$) reads

$$\frac{\partial}{\partial z} \left[c_{44} \left(e^{(1)} + \frac{\partial u}{\partial z} \right) + c_{46} \frac{\partial u}{\partial x} \right] + \frac{\partial}{\partial x} \left[c_{66} \left(e^{(2)} + \frac{\partial u}{\partial x} \right) + c_{46} \frac{\partial u}{\partial z} \right] = \rho \frac{\partial^2 u}{\partial t^2}, \quad (16)$$

$$\left[1 - \frac{\tau_\epsilon^{(1)}}{\tau_\sigma^{(1)}} \frac{\partial u}{\partial z} - \frac{e^{(1)}}{\tau_\sigma^{(1)}} \right] = \frac{\partial e^{(1)}}{\partial t}, \quad (17)$$

$$\left[1 - \frac{\tau_\epsilon^{(2)}}{\tau_\sigma^{(2)}} \frac{\partial u}{\partial x} - \frac{e^{(2)}}{\tau_\sigma^{(2)}} \right] = \frac{\partial e^{(2)}}{\partial t}. \quad (18)$$

The above system of equations may be solved efficiently in the time-domain by using a spectral method (Carcione and Cavallini, 1993b). We now apply this scheme to two typical examples.

NUMERICAL SIMULATIONS

First computer experiment.- The values of the high-frequency elastic constants and density are taken as $c_{44} = 6.8$ GPa, $c_{66} = 3.8$ GPa, and $c_{46} = 1.5$ GPa, and $\rho = 1.364$ Kg/m³, respectively. The relaxation peaks of both dissipation mechanisms are centered at $f_0 = 1/(2\pi\tau_0^{(m)}) = 10$ Hz, and the values of the minimum quality factors along the vertical (z) and horizontal (x) directions are $Q_0^{(1)} = 5$ and $Q_0^{(2)} = 20$ respectively. The modeling algorithm solves for wave propagation with a source central frequency of 10 Hz. Along the vertical direction, Figures 1a and 1b represent the quality factor and the wave velocities, respectively. As can be seen, the quality factor has its minimum value at 10 Hz, the frequency for which the group velocity has the maximum deviation from the energy and envelope velocities. In the low and high-frequency (elastic) limits, the three velocities coincide. The pictures shown in Figure 2 are snapshots, with different graphical representations, taken at 250 ms propagation time. Figure 2a shows the displacement u , and Figure 2b displays $|u|^2$, which, roughly speaking, represents the energy location. The thick continuous line is the theoretical high-

frequency energy velocity (multiplied by 250 ms), which coincides with the onset of the wavefield. In particular, this coincidence is clear in Figure 2a. This curve gives the elastic wave surface (Herrera and Gurtin, 1965). In Figure 3, we compare a numerical (white dots) and a theoretical (continuous line) evaluation of the energy location at a frequency of 10 Hz. The numerical evaluation of the energy location is obtained by finding the center of gravity of $|u|^2$ along the radial direction. The continuous line is calculated from the following equation:

$$d = V_e(t_s - t_0),$$

where d is the distance from the source, $t_s = 250$ ms, and t_0 is half the source duration. Alternatively, this comparison can be performed using the Cartesian plot in Figure 4, where the envelope and group velocities are also represented. While the envelope and energy velocities coincide practically, the group velocity gives a wrong prediction of the energy location, thus failing to represent any physical (measurable) quantity.

Second computer experiment.- A medium can be strongly anisotropic in the unrelaxed high-frequency limit, and yet behave isotropically at a given finite frequency. This behavior is demonstrated by the following example. Consider an orthorhombic solid with $c_{44} = 6.8$ GPa, $c_{66} = 4.8$ GPa, $\rho =$

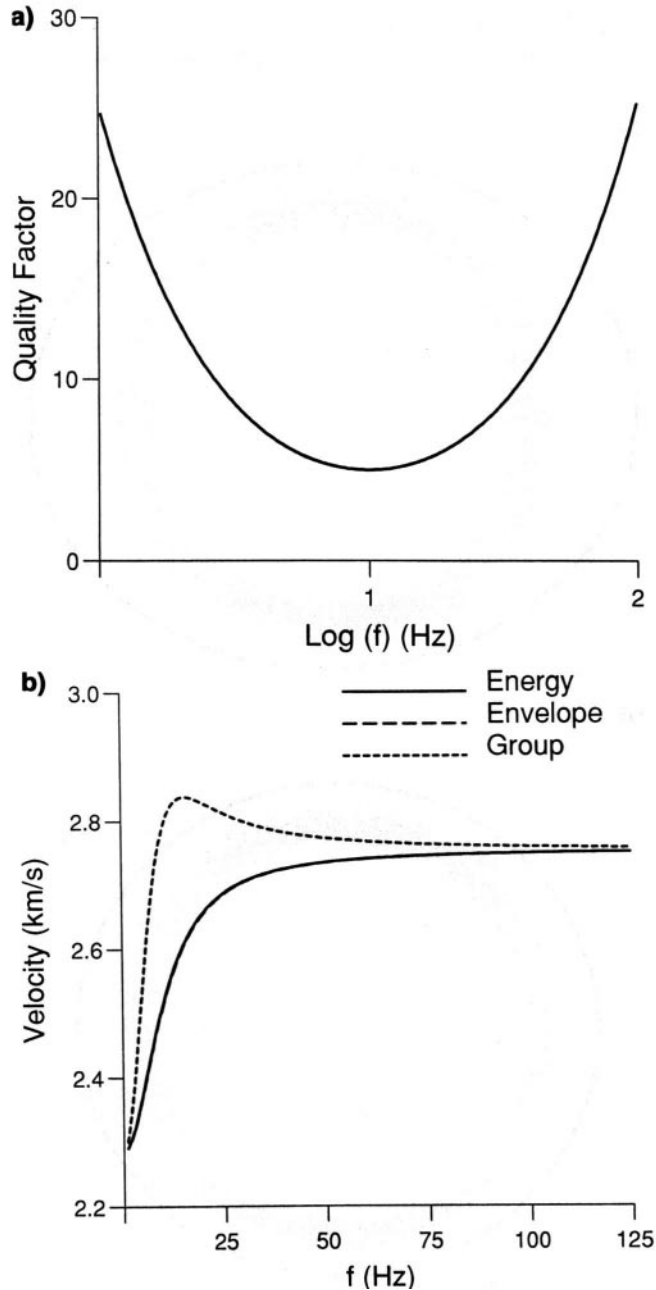


FIG. 1. Quality factor (a), and wave velocities (b), versus frequency. The propagation direction is downward vertical (i.e., along the negative z-semiaxis). The quality factor has its minimum value at 10 Hz, where the group velocity has a maximum deviation from the energy and envelope velocities.

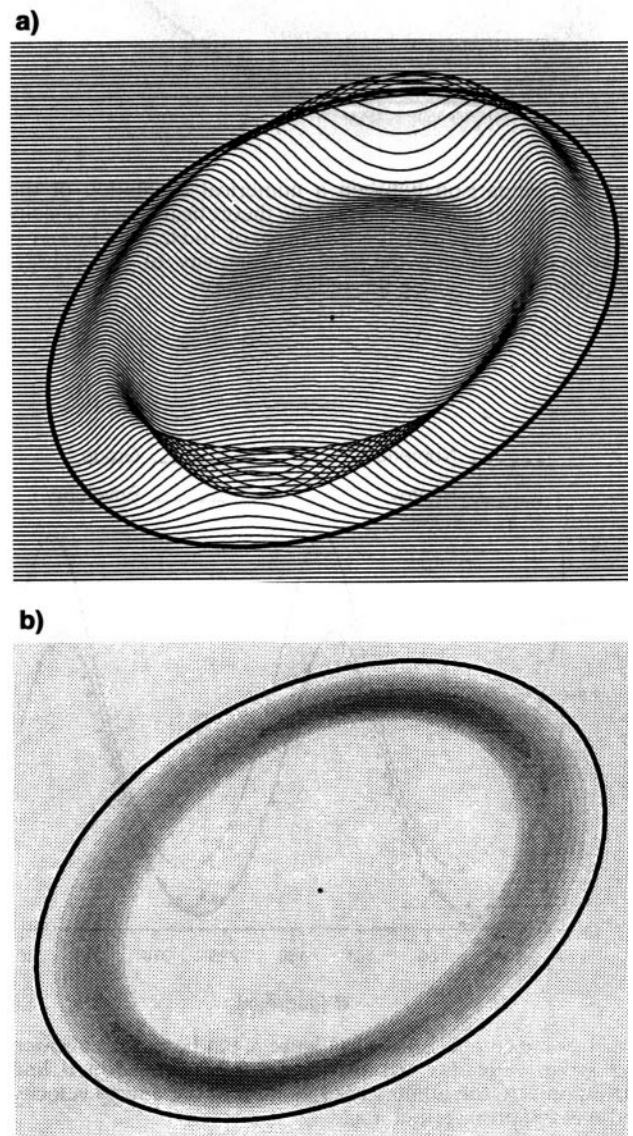


FIG. 2. Snapshots of numerically simulated wavefields taken at time $t = 250$ ms: (a) snapshot of the displacement u , (b) snapshot of the energy-like quantity $|u|^2$. The thick continuous line is the theoretical high-frequency limit energy velocity (multiplied by 250 ms).

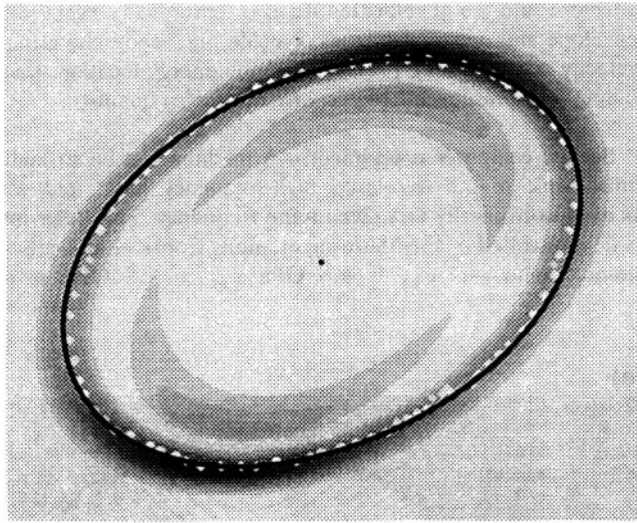


FIG. 3. Comparison between a numerical evaluation of the energy location (white dots) and the theoretical energy velocity curve (continuous line) at a frequency of 10 Hz. The former is computed by finding the center of gravity of the energy-like quantity $|\mathbf{u}|^2$ along the radial direction.

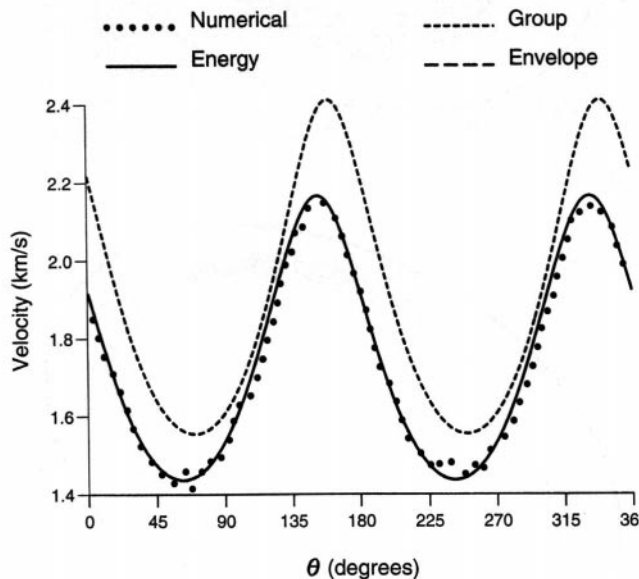


FIG. 4. Same comparison as in Figure 3, but here, the envelope and group velocities are also represented. The dotted line corresponds to the numerical evaluation of the energy velocity and θ is the propagation angle.

1.364 gr/cm³, $Q_0^{(1)} = 3$, and $Q_0^{(2)} = 20$. As before, the source central frequency is 10 Hz. Figure 5 represents the snapshot of $|\mathbf{u}|^2$ and the unrelaxed (a), and 10 Hz (b), theoretical energy velocity (scaled) curves. As can be seen, the snapshot reveals the almost perfect cylindrical symmetry of the wave. The anisotropic character of the medium emerges from the anisotropic attenuation and width of the wavefield (dynamical effects), although these effects are more difficult to measure, in practice, than are variations of wave velocities (kinematic effects) caused by elastic anisotropy and/or directional dissipation.

CONCLUSIONS

Results from numerical modeling in homogeneous dissipative anisotropic media agree with the plane-wave theory based

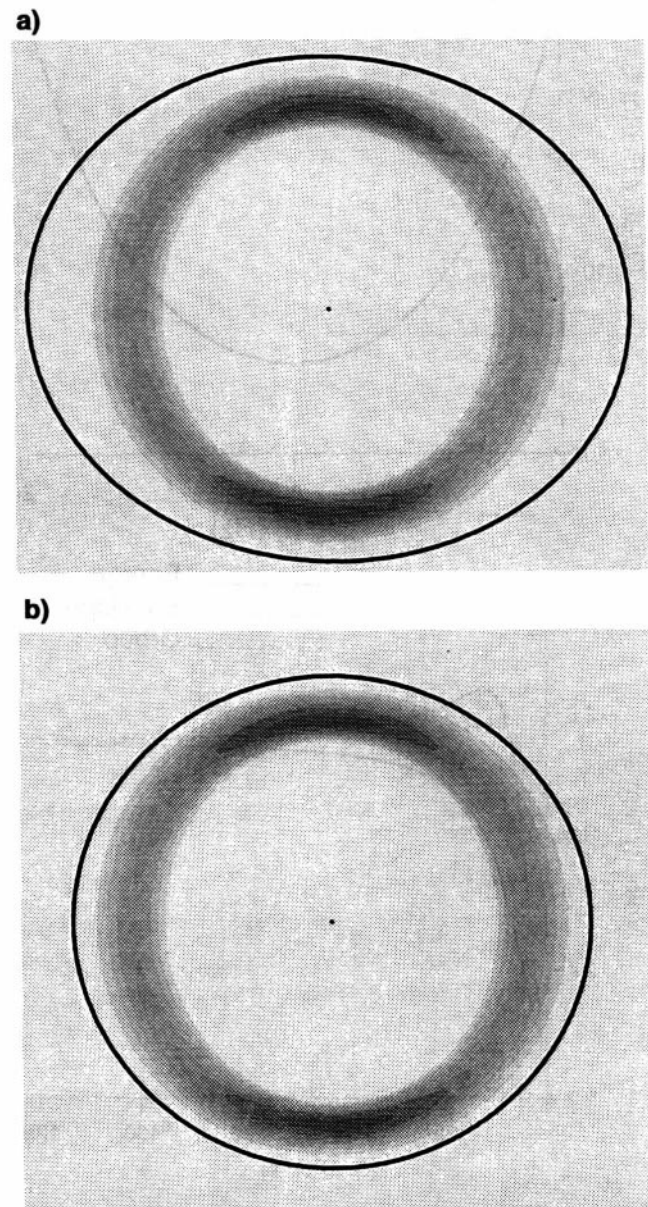


FIG. 5. Snapshots of the energy-like quantity $|\mathbf{u}|^2$ in a strongly anisotropic orthorhombic medium. The source central frequency is 10 Hz. The continuous lines are the theoretical energy velocities: at (a) infinite frequency, and at (b) 10 Hz.

on homogeneous, viscoelastic plane waves. The energy velocity effectively defines the location of the energy, while the group velocity gives a wrong prediction. As a further conclusion, the results suggest that the transient wavefield in a homogeneous medium can be viewed as a linear superposition of homogeneous viscoelastic plane waves.

Moreover, our second example shows the paradoxical result that a medium which is strongly anisotropic in the unrelaxed (elastic) limit may behave almost isotropically at an intermediate frequency. Therefore, in dissipative anisotropic media, material symmetry may not be detected through wave propagation experiments or inversion algorithms that are based solely on kinematic effects. Amplitude information (dynamical effects) may be helpful in reducing the uncertainty.

ACKNOWLEDGMENTS

This work was funded in part by the European Commission in the framework of the JOULE programme, sub-programme Advanced Fuel Technologies.

REFERENCES

- Arts, R., 1993, A study of general anisotropic elasticity in rocks by wave propagation. Theoretical and experimental aspects: Ph.D thesis, Univ. of Paris.
- Carcione, J. M., 1990, Wave propagation in anisotropic linear viscoelastic media: theory and simulated wavefields: *Geophys. J. Internat.*, 101, 739-7501
- 1994, Wavefronts in dissipative anisotropic media: *Geophysics*, 59, 644-657.
- Carcione, J. M., and Cavallini, F., 1993a, Energy balance and fundamental relations in anisotropic viscoelastic media: *Wave Motion*, 18, 1-20.
- 1993b, Modeling anelastic shear waves in the symmetry plane of a monoclinic medium: Presented at SEG/CPS Beijing Internat. Geophys. Conference and Exposition.
- Herrera, I., and Gurtin, M. E., 1965, A correspondence principle for viscoelastic wave propagation: *Quart. Appl. Math.*, 22, 360-364.
- Hosten, B., Deschamps, M., and Tittmann, B. R., 1987, Inhomogeneous wave generation and propagation in lossy anisotropic solids. Applications to the characterization of viscoelastic composite materials: *J. Acoust. Soc. Am.*, 82, 1763-1770.
- Le, L. H. T., Krebes, E. S., and Quiroga-Goode, G. E., 1994, Synthetic seismograms for SH-waves in anelastic transversely isotropic media, *Geophys. J. Int.*, 116, 598-604.